The Italian Ship Model Basin

Technical Report 2002-049

Theoretical Formulations and Numerical Methods for the Prediction of Noise from Rotating Blades

S. Ianniello
E. De Bernardis

December 2002

ISTITUTO NAZIONALE PER STUDI ED ESPERIENZE DI ARCHITETTURA NAVALE

Via di Vallerano 139
I-00128 Roma
ITALY
www.insean.it

Contents

Introduction 1

I Theoretical foundation 2

1 Historical overview 2

2 The governing equations 3

3 The solution of the governing wave equations 6

3.1 The quadrupole noise 8

3.2 The surface noise 9

II Application in aeroacoustics and hydroacoustics 11

4 Aeroacoustics of helicopter rotor 11

4.1 Linear aeroacoustics problems 12

4.2 Non-linear aeroacoustics problems 14

5 Hydroacoustics of marine propeller 17

III Conclusions 21

6 Concluding remarks on theoretical formulas 22

7 Considerations on computational noise prediction 22

Acknowledgements 23

References 23

List of Figures

1 Noise predictions of a four-bladed rotor at hover (top) and level flight (bottom) conditions (pressure in Pascal, one revolution period). 13

2 BVI noise prediction for a 6° descent case (units as in the previous). 13

3 Examples of PNL (Perceived Noise Level) contour plots for a complete helicopter configuration in level flight (left) and climb (right) conditions. 14

4 Comparison between the CAA (Euler) and the predictions based on the FWH equation for the UH-1H hovering rotor blade at M_{tip}=0.85 (non-delocating shock). 16

5 HSI noise prediction for the UH-1H hovering rotor blade at $M_{tip} = 0.90$ (delocating shock) using the K-Algorithm and the integration on a supersonic emission surface. 16

6 Three-dimensional view of the computational grid for the DTRC 4148 propeller and schematic of the microphone locations (with corresponding coordinates) for noise prediction tests. 19

7 Comparison between noise predictions for cavitating and non-cavitating conditions: thickness (left), loading (center) and overall (right) signatures, at in-plane microphone locations 1 (top) and 2 (bottom). 19

8 Comparison between noise predictions for cavitating and non-cavitating conditions: thickness (left), loading (center) and overall (right) signatures, at off-plane microphone locations 3 (top) and 4 (bottom). 20

9 Comparison between predicted overall noise spectra for cavitating and non-cavitating conditions at the four microphone locations. 21

Introduction

The purpose of this paper is to provide a complete view of methods for the prediction of noise generated by rotating blade devices, based on the solution of the wave equation. Analysis and results from numerous papers are reported to present the historical development and the state of the art in the field of open rotor acoustics.

Several alternative methods have been developed and tested successfully over the last decade for the study of rotor aeroacoustics. Most are based on direct solution of balance equations to determine the flow field and this branch is known as Computational aeroacoustics (CAA). Although several attractive features of boundary integral solutions of the wave equation still make them the standard approach to the prediction of noise from rotating blade, a proper integration of the different methodologies, is progressively showing as the best strategy.

The authors' main experience is in the study of aerodynamic noise generated by aircraft propellers and helicopter rotors, but their current involvement and future activities are mostly devoted to the analysis of hydrodynamic noise from marine propellers. The presentation of some results benefits from this broadband expertise and covers phenomenological aspects of aeroacoustics and hydroacoustics.

From a methodological standpoint, the emphasis is on theoretical formulations based on integral representation of the sound field: the computational application presented always refers to the treatment of these formulas in the time domain. The guidelines of the scientific overview to these mathematical tools are due to Farassat, who presented an excellent paper on the subject last year [1].

Two linear wave equations, the Kirchhoff (KHF) and the Ffowcs Williams-Hawkings (FWH) equations are first presented. The approach of Ffowcs Williams and Hawkings can be considered as a Kirchhoff method. Actually, they call one of their result as the extension of the Kirchhoff formula to a moving surface. The solution of the KHF equation, leading to the Kirchhoff formula for moving surfaces, and the relation of the KHF equation to the FWH equation are then shown. Finally, the solution of several wave equations, characterized by different forms of source terms, is discussed.

The paper is organized as follows. In section 1 a short overview is given on the historical development of methods for the prediction of noise from rotating blades. In section 2 the governing equations of the Kirchhoff method are presented. Here two equations called the KHF and the FWH equations are derived. Four inhomogeneous source terms are recognized in these equations. In Section 3, it is shown how to obtain the solutions to the wave equations with the different source terms. Application of the theoretical results to the calculation of noise from helicopter rotors and marine propellers is thus presented in sections 4 and 5.

Part I

Theoretical foundation

1 Historical overview

Early steps of propeller noise prediction date back to Gutin's formula [2] in the 1930s. This formula is for rotating compact dipoles and predicts the loading noise only. Thickness noise prediction was ignored because there was a feeling that it was not important. This was contrary to the conclusion of Ernsthausen [3] and Deming [4, 5] who investigated thickness noise in the same period. Deming had derived a thickness noise formula following the analytic procedure of Gutin. He also presented numerical results supporting experimental data on the importance of thickness noise at high blade tip speeds.

In the early Seventies, most noise prediction methods were in the frequency domain. This was the natural approach for the researchers because time domain methods generally require powerful computers. By suitable approximation and ingenuity, closed form solutions were obtained for some significant problems using the frequency domain analysis. Lowson [6] had developed helicopter noise prediction codes based on his theory. He had shown the consistency of his result with that of Gutin. Aeroacoustics was an active research area and many experimental and theoretical works were being published then. Lighthill's theory of acoustic analogy [7] was extended to flows in the presence of fixed and moving surfaces by Curle [8] and Ffowcs Williams and Hawkings [9], respectively.

The availability of powerful computers, and progress in computational fluid dynamics, as well as the development of more versatile measuring instruments, helped significantly in advancement of the time domain method. Also, the progress in solving partial differential equations, particularly the use of the theory of distributions or generalized functions [10, 11, 12], made it possible to get closed form solution of the wave equation with sources on a moving surface in various forms suitable for noise prediction. Ffowcs Williams and Hawkings had used generalized function theory in their work. The power of this theory is such that much of what was known before such as the Kirchhoff formula for radiation [13], as well as the formulas of Curle and Lowson, can be derived and extended. Other issues — such as the role played in noise generation by specific phenomena arising in high speed flow in air (shock waves) and water (cavitation) — can naturally be addressed using this theory.

Goldstein has used basic generalized function theory to derive some of the important results of aeroacoustics [14]. Farassat has then covered the details of the mathematics used for the wave equation with sources on a moving surface [15, 16].

2 The governing equations

The classical Kirchhoff formula [13] provides the solution of the wave equation outside a surface S in terms of a surface integral over S, the so-called data surface. The integrand depends on the values of the unknown function, its normal and time derivatives on S. It can be obtained by an elegant method which requires some concepts in generalized functions. The unknown function, say the acoustic pressure, is extended to the interior of the surface by assuming that its value is zero there. Then the wave operator is applied to this discontinuous function treating all the derivatives as generalized derivatives [10, 11, 12, 15, 16]. Source terms are thereby generated, giving rise to an inhomogeneous wave equation which involve the Dirac delta function with its support on the surface S. This inhomogeneous wave equation is called the KHF equation.

Using the Green's function of the wave equation in the unbounded space to formally solve the KHF equation will give the Kirchhoff formula. One is not restricted to a stationary data surface in this approach. This is precisely the method that Farassat and Myers used to derive the Kirchhoff formula for a moving surface [16, 17]. The same idea of extending all fluid parameters to the interior of the surface S was utilized by Ffowcs Williams and Hawkings to get the FWH equation. They used the mass and momentum conservation laws treating all the derivatives as generalized derivatives and manipulated these two equations as Lighthill did to obtain a wave equation [9, 12, 14, 15]. Interesting relationships between the use of KHF and FWH equations concern the selection and use of the (moving) surface where data are prescribed [18, 19]. However, in deriving the KHF equation, it is assumed that the unknown function satisfies the linear wave equation everywhere while the FWH equation utilizes the conservation laws. This explains the difference in behavior of the solutions of these equations in the near field.

Consider a moving surface described by $f(\mathbf{x}, t) = 0$ such that $f > 0$ outside the surface and $|\nabla f| = 1$ on the surface. Let p' be the acoustic pressure. Then the KHF equation is easily derived in the form [15, 16, 17]:

$$\bar{\Box}^2 \tilde{p}'(\mathbf{x}, t) = -\left[\frac{\partial p'}{\partial n} + \frac{M_n}{c_0}\frac{\partial p'}{\partial t}\right]\delta(f) - \frac{1}{c_0}\frac{\bar{\partial}}{\partial t}M_n p'\delta(f) - \frac{\bar{\partial}}{\partial x_i}p' n_i \delta(f) \qquad \text{(I.1)}$$

where

$$\tilde{p}' = \begin{cases} p', & f > 0 \\ 0, & f < 0 \end{cases} \qquad \text{(I.2)}$$

p'_n and p'_t are the normal and time derivatives of p', respectively, M_n is the local normal Mach number of the surface, c_0 is the speed of sound and $\mathbf{n} = \nabla f$ is the unit, outward pointing, normal to the surface. Using the Green's function of the wave equation in the unbounded space gives the solution of the KHF equation. This is the Kirchhoff formula for the moving surface $f = 0$ [15, 16, 17].

The FWH equation is [9, 12, 15, 20]:

$$\begin{aligned}\bar{\Box}^2 p'(\mathbf{x},t) &= \frac{\bar{\partial}^2}{\partial x_i \partial x_j} T_{ij} H(f) \\ &- \frac{\bar{\partial}}{\partial x_i} P_{ij} n_j \delta(f) \\ &+ \frac{\bar{\partial}}{\partial t} \rho_0 v_n \delta(f) \end{aligned} \tag{I.3}$$

The FWH equation can be derived by embedding the exterior flow problem in unbounded space by using generalized functions to describe the flow field. The mathematical procedure proposed here is due to Farassat [15]. Consider again a moving surface $f(\mathbf{x},t) = 0$, with a stationary fluid outside, and defined so as to make $\nabla f = \mathbf{n}$, where $\mathbf{n}$ is a unit normal vector pointing outward. Inside the surface, the generalized flow variables are defined so as to have their free-stream values, that is:

$$\tilde{\rho} = \begin{cases} \rho, & f > 0 \\ \rho_0, & f < 0 \end{cases} \tag{I.4}$$

$$\widetilde{\rho u_i} = \begin{cases} \rho u_i, & f > 0 \\ 0, & f < 0 \end{cases} \tag{I.5}$$

$$\tilde{P}_{ij} = \begin{cases} P_{ij}, & f > 0 \\ 0, & f < 0 \end{cases} \tag{I.6}$$

where the tilde indicates that the variable is a generalized function defined through the whole space. In the above, ρ, ρu_i are the density and momentum, respectively, while $P_{ij} = E_{ij} + (p - p_0)\delta_{ij}$ are the components of the (compressive) stress tensor, with E_{ij} components of the viscous stress tensor. By using definitions in (I.4), (I.5) and (I.6), a generalized continuity equation can be written as follows:

$$\frac{\bar{\partial}\tilde{\rho}}{\partial t} + \frac{\bar{\partial}}{\partial x_i}(\widetilde{\rho u_i}) = \left[(\rho - \rho_0)\frac{\partial f}{\partial t} + \rho u_i \frac{\partial f}{\partial x_i} \right] \delta(f) \tag{I.7}$$

where the bar over the derivative operators denotes differentiation in the sense of generalized functions [12]. Also note that

$$\frac{\partial f}{\partial t} = -v_n, \quad \frac{\partial f}{\partial x_i} = n_i$$

while $\delta(f)$ is the Dirac delta function. The generalized momentum equation can be written:

$$\frac{\bar{\partial}}{\partial t}(\widetilde{\rho u_i}) + \frac{\bar{\partial}}{\partial x_j}(\widetilde{\rho u_i u_j}) + \frac{\bar{\partial}\tilde{P}_{ij}}{\partial x_j} = \left[\rho u_i \frac{\partial f}{\partial t} + (\rho u_i u_j + P_{ij}) \frac{\partial f}{\partial x_j} \right] \delta(f) \tag{I.8}$$

If one takes the generalized time derivative of equation (I.7), the generalized divergence of equation (I.8), subtracts the latter from the former and rearranges the result by subtracting

$$c_0^2 \delta_{ij} \frac{\bar{\partial}^2 \rho}{\partial x_i \partial x_j},$$

one finally gets

$$\begin{aligned} \bar{\Box}^2 p'(\mathbf{x},t) &= \frac{\bar{\partial}^2}{\partial x_i \partial x_j}\left[T_{ij} H(f)\right] \\ &- \frac{\bar{\partial}}{\partial x_i}\left\{\left[P_{ij} n_j + \rho u_i (u_n - v_n)\right]\delta(f)\right\} \\ &- \frac{\bar{\partial}}{\partial t}\left\{\left[\rho_0 v_n + \rho(u_n - v_n)\right]\delta(f)\right\} \end{aligned} \tag{I.9}$$

where

$$\bar{\Box}^2 = \frac{1}{c_0^2}\frac{\bar{\partial}^2}{\partial t^2} - \bar{\nabla}^2$$

is the generalized wave operator, with c_0 the sound speed in quiescent medium. In the left-hand side, $p' = c_0^2 \rho'$ is the acoustic pressure disturbance: this means it is assumed that the observer be outside the source region, where the only disturbance is assumed to be the (isentropic) propagating sound field. In the right-hand side, T_{ij} is the Lighthill stress tensor: $T_{ij} = \rho u_i u_j + E_{ij} + (p - p_0) - c_0^2(\rho - \rho_0)\delta_{ij}$), while $H(f)$ is the Heaviside function. Also, u_n is the fluid velocity in the direction normal to the surface $f = 0$ and v_n is the surface velocity in the direction normal to the surface itself. In the applications of the FWH equation, the surface $f = 0$ is generally assumed to be coincident with the (impenetrable) body surface, which implies $u_n = v_n$. This provides the final form of the FWH equation (I.3).

There are four types of source terms in the KHF and FWH equations. One needs to find the solution for the following four types of wave equations:

$$\bar{\Box}^2 p'(\mathbf{x},t) = \frac{\bar{\partial}^2}{\partial x_i \partial x_j} T_{ij} H(f) \tag{I.10}$$

$$\bar{\Box}^2 p'(\mathbf{x},t) = -\left[\frac{\partial p'}{\partial n} + \frac{M_n}{c_0}\frac{\partial p'}{\partial t}\right]\delta(f) \tag{I.11}$$

$$\bar{\Box}^2 p'(\mathbf{x},t) = \frac{\bar{\partial}}{\partial t}\rho_0 v_n \delta(f) \tag{I.12}$$

$$\bar{\Box}^2 p'(\mathbf{x},t) = -\frac{\bar{\partial}}{\partial x_i} P_{ij} n_j \delta(f) \tag{I.13}$$

This approach has several advantages. First the solution of each of these equations are basically different. Second, by seeking exact closed form solutions of these equations, one is able to evaluate various kinds of common approximations used in practical problems. No approximations have been made to the blade geometry and kinematics in the derivation of the main formulations.

3 The solution of the governing wave equations

It is now described how to obtain the solution of equations (I.10-I.13) are solved. Several papers deal with the issues treated hereafter. A complete though concise presentation can be found in [15] It is not possible to give all the relevant details here because the algebraic manipulations are somewhat extensive.

Different techniques can be used to obtain a formal solution of the wave equation, that is an integral expression for the acoustic pressure p' at given observer location and time. Even in this case, the use of generalized function theory leads to important results. A brief summary is given here of the integration of a wave equation with source term like those appearing in the FWH and the KHF equations.

The Green's function for the wave equation in the unbounded space (accounting for the Sommerfeld radiation condition) is [21, 22, 23]:

$$G(\mathbf{y},\tau;\mathbf{x},t) = \begin{cases} \delta(g)/4\pi r & (\tau \le t) \\ 0 & (\tau > t) \end{cases} \tag{I.14}$$

where

$$g = \tau - t + \frac{r}{c_0}$$

In this equation, $(\mathbf{x}, t)$ and $(\mathbf{y}, \tau)$ are the observer and the source space-time variables, respectively, while $r = |\mathbf{x} - \mathbf{y}|$.

It can be seen that equation (I.3), considering their source terms separately, can be referred to the two standard forms:

$$\overline{\Box}^2\phi = Q(\mathbf{x},t)H(f) \tag{I.15}$$

$$\overline{\Box}^2\phi = Q(\mathbf{x},t)\delta(f) \tag{I.16}$$

In the first case, the source is distributed through a three-dimensional portion of space, while the expression (I.16) denotes a source distributed on the moving surface $f = 0$.

The solution of equation (I.15) can be written in different forms, starting with the expression:

$$4\pi\phi(\mathbf{x},t) = \int_{f>0} Q(\mathbf{y},\tau)\frac{\delta(g)}{r}\,d\tau\,d\mathbf{y}$$

The most widely used in applications is that directly obtained performing the integration on τ, using the definition of g, that is

$$4\pi\phi(\mathbf{x},t) = \int_{F>0} \frac{[Q(\mathbf{y},\tau)]_{\text{ret}}}{r}\,d\Omega(\mathbf{y}) \tag{I.17}$$

where the subscript "ret" means that the values of the source function are to be taken at the corresponding retarded time $\tau = t - r/c_0$, that is at $g = 0$, while $F(\mathbf{y}; \mathbf{x}, t) = [f(\mathbf{y}, \tau)]_{\text{ret}} = f(\mathbf{x}, t - r/c_0)$, and where $d\Omega$ is the volume element of the space region $F > 0$.

Two different forms are given now for the solution of equation (I.16). The formal Green's function solution is:

$$4\pi\phi(\mathbf{x}, t) = \int Q(\mathbf{y}, \tau)\delta(f)\frac{\delta(g)}{r}\, d\tau\, d\mathbf{y} \tag{I.18}$$

To get the first form, the above equation is integrated as follows. A lagrangian variable η is introduced on and near the surface $f = 0$, such that the Jacobian of the transformation $\mathbf{y} \Rightarrow \eta$ is unity. Note that $\mathbf{y} = \mathbf{y}(\eta, \tau)$, and

$$r = |\mathbf{x} - \mathbf{y}(\eta, \tau)|. \tag{I.19}$$

Noting that for a rigid surface $f = 0$, with a local velocity $\mathbf{v}$, one can define:

$$M_r = \frac{\mathbf{v}}{c_0} \cdot \frac{\mathbf{r}}{r}$$

the local Mach number in the radiation direction, the integration of (I.18) may be achieved through the transformation $\tau \Rightarrow g$, for which

$$\frac{\partial g}{\partial \tau} = 1 - M_r.$$

The integration of $\delta(g)$ and $\delta(f)$ (taking into account that $|\nabla f| = 1$), eventually leads to:

$$4\pi\phi(\mathbf{x}, t) = \int_{f=0} \left[\frac{Q(\eta, \tau)}{r|1 - M_r|}\right]_{\text{ret}} dS(\eta) \tag{I.20}$$

A different method of integrating the delta functions in equation (I.18) is to let $\tau \Rightarrow g$ and integrate with respect to g. This gives:

$$4\pi\phi(\mathbf{x}, t) = \int \frac{1}{r}\, [Q(\mathbf{y}, \tau)]_{\text{ret}}\, \delta(F)\, d\mathbf{y} \tag{I.21}$$

Note that, although $|\nabla f| = 1$ has been defined, one has $|\nabla F| \neq 1$ in general. It is easily shown that

$$|\nabla F| = \left(1 + M_n^2 - 2M_n \cos\theta\right)^{\frac{1}{2}} \equiv \Lambda \tag{I.22}$$

where $M_n = v_n/c_0$ and $\cos\theta = \mathbf{n} \cdot \mathbf{r}/r$ is the cosine of the angle between the local normal to $f = 0$ and the radiation direction. Using equation (I.22) in equation (I.21), one gets:

$$4\pi\phi(\mathbf{x}, t) = \int_{F=0} \frac{1}{r} \left[\frac{Q(\mathbf{y}, \tau)}{\Lambda}\right]_{\text{ret}} d\Sigma(\mathbf{y}) \tag{I.23}$$

where $d\Sigma$ is the element of the surface area on $F = 0$.

3.1 The quadrupole noise

The quadrupole noise is governed by equation (I.10). This term only appears in the FWH equation. Ideally, one would like to locate the data surface where the contribution of the quadrupoles outside the surface to the noise is small. At present in some important problems, such as in high speed helicopter rotor noise prediction, this does not seem possible because the accuracy of the CFD data is not satisfactory where the data surface must be positioned. The alternative technique is taking the blade surface as the data surface and adding the contribution of the quadrupoles in the regions where they have large source strength, to the surface noise. This requires a suitable solution of equation (I.10) as well as a good approximation method based on the physics of the problem. Some exact results will first be presented.

Let $(\mathbf{x}, t)$ and $(\mathbf{y}, t)$ be the observer and the source space-time variables. For $r = |\mathbf{x} - \mathbf{y}|$, the surface defined by $g = 0$, that is $r - c_0(t - \tau) = 0$ identifies a sphere with center at the observer and the radius $c_0(t - \tau)$ for all $\tau \leq t$. Here c_0 is the speed of sound in the undisturbed medium. Besides, $F(\mathbf{y}; \mathbf{x}, t) = f(\mathbf{y}, \tau)_{\text{ret}} \equiv f(\mathbf{y}, t - r/c_0)$. The solution of equation (I.10) is

$$4\pi p'(\mathbf{x}, t) = \frac{\partial^2}{\partial x_i \partial x_j} \int_{F>0} \frac{T_{ij\,\text{ret}}}{r} d\Omega(\mathbf{y}) \tag{I.24}$$

One can visualize the above integral dynamically. In what follows, it is assumed that $(\mathbf{x}, t)$ is kept fixed in the discussion. The surface $g = 0$ is called the collapsing sphere because, this surface represents a sphere with center at $\mathbf{x}$ whose radius collapses at speed of sound. The surface $F = 0$ is generated by the intersection of the collapsing sphere and the data surface $f = 0$ for $\tau \leq t$. This surface can be determined for a fixed $(\mathbf{x}, t)$ in advance and is independent of the source time. The volume integral in equation (I.24) sums the contribution of all the quadrupoles outside the surface $F = 0$ at the source time τ. The result of the integral is, therefore, a function of $(\mathbf{x}, t)$.

The above integral treats all the quadrupoles as volume sources. It is an exact result and is valid even when shock waves, wakes and other discontinuities are present in the flow. In practical problems, the integral on the right side of equation (I.24) is evaluated numerically and one is therefore obliged to use numerical differentiation with respect to the observer variables – a procedure that is subject to numerical errors in addition to being time consuming on a computer. Farassat and Brentner [24] have converted the above double differentiation with respect to the space variables to derivatives with respect to observer time variable. The conversion can be performed exactly.

3.2 The surface noise

The starting point is giving a solution of equation (I.16) in the form of equation (I.20). The solution of equations (I.12) and (I.13) are thus obtained by using the appropriate expressions of the source terms, including differentiation.

3.2.1 The subsonic case

The solution of equation (I.12) for a data surface that moves subsonically can be written as

$$4\pi p'(\mathbf{x},t) = \frac{\partial}{\partial t}\int_{f=0}\left[\frac{\rho_0 v_n}{r|1-M_r|}\right]_{\text{ret}} dS \tag{I.25}$$

The solution of equation (I.13) is:

$$4\pi p'(\mathbf{x},t) = -\frac{\partial}{\partial x_i}\int_{f=0}\left[\frac{P_{ij}n_j}{r|1-M_r|}\right]_{\text{ret}} dS \tag{I.26}$$

In the application of this result, the space derivative is usually converted to a time derivative. This step was proposed by Farassat [25, 26], based on an identity relating the space and time derivatives of the Green's function of the Wave equation. The resulting formula is:

$$4\pi p'(\mathbf{x},t) = \frac{1}{c_0}\frac{\partial}{\partial t}\int_{f=0}\left[\frac{P_{ij}n_j}{r|1-M_r|}\right]_{\text{ret}} dS + \int_{f=0}\left[\frac{P_{ij}n_j\hat{r}_i}{r^2|1-M_r|}\right]_{\text{ret}} dS \tag{I.27}$$

where $\hat{r}_i = r_i/r = (x_i - y_i)/r$. Equations (I.25) and (I.27) give the thickness and loading noise terms of Formulation 1 of Farassat, respectively [25, 26, 27]. The data surface is taken as the blade surface itself.

The time derivative can be taken inside the integrals using the following formula, given for a generic integrand $q(\mathbf{y},\tau)$:

$$\frac{\partial}{\partial t}\left[q(\mathbf{y},\tau)\right]_{\text{ret}} = \left\{\frac{1}{|1-M_r|}\frac{\partial}{\partial \tau}\left[q(\mathbf{y},\tau)\right]\right\}_{\text{ret}} \tag{I.28}$$

When the result given by equation (I.28) is used in equations (I.25) and (I.27), the thickness and loading noise terms of Formulation 1A of Farassat are obtained [27, 28].

3.2.2 The supersonic case

For supersonically moving surfaces equations (I.25) and (I.27) cannot be used, due to the singularity arising when $M_r = 1$. In noise prediction codes, the data surface is divided into panels and the contribution of each panel to the noise is evaluated separately and summed. For panels moving at subsonic speed, the simple subsonic formulations such as 1A discussed above, equations (I.25) and (I.27), can be used.

The solution of the FWH and equation for sources on a panel moving at supersonic speed is based on the alternative integral representation of the sound field given in section 3. The thickness and loading noise terms of Formulation 1A of Farassat can be written in this case as follows:

$$4\pi p'(\mathbf{x},t) = \frac{\partial}{\partial t}\int_{F=0}\left[\frac{\rho_0 v_n}{r\Lambda}\right]_{\text{ret}} d\Sigma \tag{I.29}$$

$$4\pi p'(\mathbf{x},t) = \frac{1}{c_0}\frac{\partial}{\partial t}\int_{F=0}\left[\frac{P_{ij}n_j}{r\Lambda}\right]_{\text{ret}} d\Sigma + \int_{F=0}\left[\frac{P_{ij}n_j\hat{r}_i}{r^2\Lambda}\right]_{\text{ret}} d\Sigma \tag{I.30}$$

where Λ is defined by equation (I.22). For the above solution form of the FWH equation, the resulting analytic expression after taking all the derivatives explicitly, is a very complicated result known as the Formulation 3 of Farassat [29, 30]. Farassat and Farris [31] have recently published the full derivation of the mean curvature of the which was originally derived and published in 1996 by Farassat [16].

In propfan noise prediction, a line integral appearing in Formulation 3 can produce a logarithmic singularity in the acoustic field when the leading and trailing edges are not sufficiently swept and the propeller is operated at high supersonic tip speed. This singularity was studied by De Bernardis and Farassat [32]. Farassat and Myers [33] have shown that the singularity is removed if one adds the contribution of the quadrupoles of the FWH equation to the line integral. Thus, the singularity of the line integral in Formulation 3 is because the physics of the problem is not accounted fully in the differential equation when only the thickness and loading source terms of the FWH equation are retained.

A recent paper from a totally different direction has been given by Farassat, Brentner and Dunn [34]. They propose in this work an analytic expression for the acoustic pressure, called Formulation 4, closely related to those of geometrical acoustics and optics. Another interesting and important result is the formation of caustics in the radiation field, in particular in the near field, of rotating blades at all tip speed range. In fact, it appears that for further progress, we one should apply other areas of advanced mathematics such as the singularity theory [35] as done, for example, by Ardavan [36]. Finally, an excellent review paper was given by Lyrinzis concerning the application of Kirchhoff formulas to the prediction of rotor noise [37]).

Part II

Application in aeroacoustics and hydroacoustics

4 Aeroacoustics of helicopter rotor

An integral expression for the acoustic pressure perturbation at given observer position and time is easily derived from equation (I.3), using the results shown in section 3:

$$\begin{aligned} 4\pi p'(\mathbf{x},t) &= \frac{\partial^2}{\partial x_i \partial x_j} \int_{F>0} \frac{\left[T_{ij}\right]_{\text{ret}}}{r}\, d\Omega \\ &- \frac{\partial}{\partial x_i} \int_{F=0} \frac{1}{r} \left[\frac{P_{ij} n_j}{\Lambda}\right]_{\text{ret}} d\Sigma \\ &+ \frac{\partial}{\partial t} \int_{F=0} \frac{1}{r} \left[\frac{\rho_0 v_n}{\Lambda}\right]_{\text{ret}} d\Sigma \end{aligned} \tag{II.1}$$

This complete solution to the FWH equation is based on the "retarded configuration" technique, which is illustrated by equations (I.17) and (I.21). Actually, several forms have been developed over the years, referring also to the alternative solution method of the "material configuration", equation (I.20).

The latter has been exploited, in particular, for problems involving low speed of the rotor blades, that is when the first term above can be neglected. This leads to evaluate the second and third (linear) terms using the following expression:

$$\begin{aligned} 4\pi p'(\mathbf{x},t) = &- \frac{\partial}{\partial x_i} \int_{f=0} \left[\frac{P_{ij} n_j}{r|1-M_r|}\right]_{\text{ret}} dS \\ &+ \frac{\partial}{\partial t} \int_{f=0} \left[\frac{\rho_0 v_n}{r|1-M_r|}\right]_{\text{ret}} dS \end{aligned} \tag{II.2}$$

Formulations based on equation (II.1) are more suitable to treat problems of rotors at high tip speed, also in the transonic range with strong shock waves. Use of these technique has proven to be successful over the last few years, even in comparisons with other computational methods.

Some examples of applications are given in the following, referring to both approaches described above for the integral representation of the solution to the FWH equation. Results are presented for low-speed (linear) as well as high-speed (non-linear) rotor problems.

4.1 Linear aeroacoustics problems

The possibility of neglecting the contribution from the quadrupole source terms and the relatively simple computation of thickness and loading noise signatures make the FWH equation the standard solving approach in low speed aeroacoustics [26]. The main feature of all the integral formulations derived form the FWH equation is that the evaluation of the acoustic pressure p' at the observer time t depends on the kernel quantities computed at the retarded time $\tau = t - r/c_0 = \tau^*$; this represents the instant when the contribution of the source point was emitted from the relevant position to reach the observer location at a later time t. Two different time schemes can be adopted to evaluate the integral quantities. It is possible to assume t as the unknown and determine the noise contributions from each source point by moving forward in time; due to the different kinematic conditions of the rotating sources, a time shift exists between the signatures travelling towards the observer and the resulting noise can be obtained through an interpolation in time (*direct* method). Alternatively, by fixing an observer location and time t, it is possible to go backward in time to exactly determine the τ^* corresponding to each source point, and then evaluate the retarded integral kernels (*inverse* method).

The inverse method requires an iterative procedure to determine the emission time τ^* of each source point, but it is more accurate compared to the direct method, since at any instant all the contributions from the source points are taken into account. The reliability of the computed noise signatures strongly depends on the accuracy of the data representing the dynamics of the flow field (the pressure distribution upon the blade), and the description of the body shape and motion. For example, if a simple hovering rotor blade has to be treated a coarse grid is probably sufficient to give a satisfactory prediction of the linear terms; on the contrary, a very fine grid and a large number of time steps may be required when using the same numerical model to the analysis of a descent flight condition, characterized by a strong blade-vortex interaction and an impulsive noise waveform. In any case, a *zero-th* order formulation is usually sufficient to provide very good results; this means that, fixed a numerical discretization of the blade, each panel corresponds to a constant value of the integral kernel, considered at the panel *centroid*.

Figure 1 shows noise predictions obtained through the Farassat's formulation 1A [26] for different flight conditions; the required blade airload distributions were determined by fitting the pressure data measured on an instrumented model (the BO-105 model with 124 pressure transducers) and the signatures refer to a microphone placed below the rotor plane, where the loading noise is predominant [38]. The good agreement between the numerical predictions and the available experimental data reveals the reliability and the accuracy of the method. A larger number of pressure transducers upon the blade model and an increased resolution in time of the airload distribution during the revolution period, allow to improve this agreement in a critical BVI test case (a 6° descent flight), as reported in Figure 2 [39].

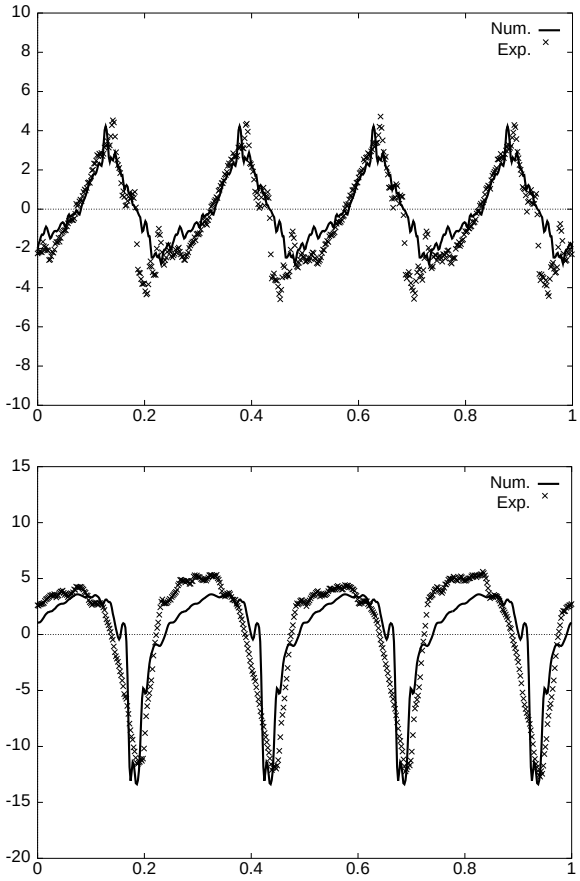

Figure 1: Noise predictions of a four-bladed rotor at hover (top) and level flight (bottom) conditions (pressure in Pascal, one revolution period).

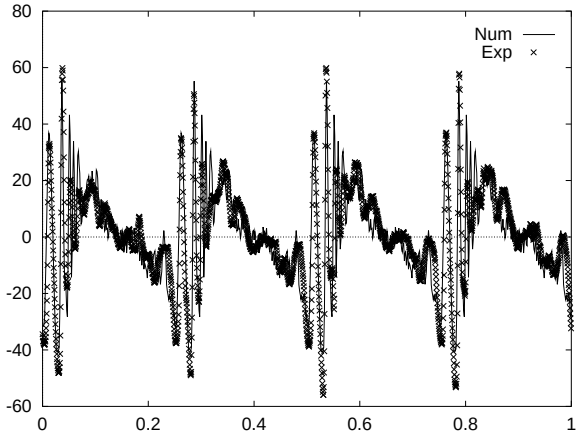

Figure 2: BVI noise prediction for a 6° descent case (units as in the previous).

A large effort is being spent within the aeroacoustics community to deal with a multibody geometry, in order to study a complete helicopter (main rotor, tail rotor and the fuselage) or the complex tilt-rotor configurations at different flight conditions. The challenging problems here are the mutual scattering of the bodies, the possible lack of periodicity of the blade airload distributions and the great deal of variables affecting the motion and the synchronism between the different components. Figure 3 shows the PNL (Perceived Noise Level) contour plots referring to level flight and climb conditions for a complete BO-105 helicopter, computed by a sophisticated FWH equation solver within the Brite-Euram HELIFLOW project [40]. The plots reveal (as expected) that at level flight the most noisy region corresponds to the advancing blade (quadrant II) while the presence of the tail rotor is clearly recognized in the rear part of the helicopter, especially in front of the rotor itself; nevertheless, a rather strange lobe in the III quadrant spreads out notably forward the body. At climb, a smaller region is affected by noise, and a lower PNL is observed.

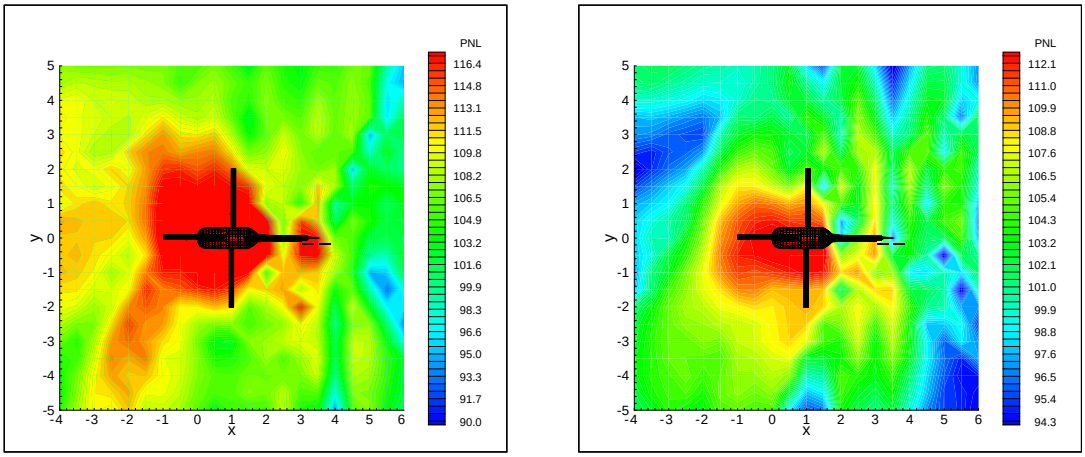

Figure 3: Examples of PNL (Perceived Noise Level) contour plots for a complete helicopter configuration in level flight (left) and climb (right) conditions.

4.2 Non-linear aeroacoustics problems

The computational simplicity of formulations based on the FWH equation disappears when dealing with problems involving transonic or supersonic speed, where the nonlinear terms play a significant role in the flow field dynamics, and then in noise generation. The presence of the quadrupole three-dimensional integrals and the non-compactness of noise sources outside the sonic cylinder make the problem modelling very complex; furthermore, the availability of a suitable set of flow data (involving the perturbation velocity field around the blade) is rather rare at the operating conditions of interest, so that for many years the attention of the aeroacousticians was focused on some alternative solution techniques as the Kirchhoff approach [37] or the Computational Aeroacoustics (CAA) [41].

Computation of nonlinear terms in the FWH equation through a volume integration was proposed in 1994 by the authors [42]; validation by experimental data as well as comparison with analogous noise prediction through CAA showed satisfactory. Figure 4 depicts results for a hovering rotor blade at M_{tip}=0.85 (a non-delocating condition) and an observer in the rotor plane, at a distance of 3.09 radii from the hub. Figure on the left shows the experimental data, the thickness noise component (dashed line) and the numerical prediction of overall noise obtained through an Euler code (solid line); figure on the right shows the separate contributions from the quadrupole term and the monopole from the solution of the FWH equation: the overall signature is in good agreement with experimental data.

The actual difficulty in computing the quadrupole contribution is the need for extending the numerical domain outside the sonic cylinder, where the possibility of singularities in the Doppler factor make the usual FWH equation solvers unreliable. From a physical standpoint, this numerical singularities are related to the possible occurrence of multiple emission times for a supersonic source point: whereas the noise signal starting at τ^* runs toward the observer the supersonically moving source emits again and (depending on the relative observer-source position) three different signatures may reach the observer simultaneously. The shock delocalization (arising at a $M_{\text{tip}} \geq 0.88$) requires to account for the contribution of supersonic sources even for blade at a subsonic tip speed.

From a theoretical point of view the problem could be simply bypassed by solving equation (II.1), where the integrals are determined on the retarded configuration of the numerical domain and the Doppler singularity does not appear in the integral kernels. This solution is hard to achieve in practice. The occurrence of multiple τ^* causes unconnected regions to appear, which temporarily link together into a single domain and subsequently disappear: no numerical code exists, which is capable to follow the evolution of the three-dimensional domain Ω. Nevertheless, the evaluation of the first term of equation (II.1) can be achieved by performing a preliminary integration of T_{ij} along a direction normal to the blade ("far-field approximation" [43]); thus the integration domain collapses into a surface corresponding to the projection of Ω on the rotor plane.

At present, only two algorithms can accurately model a supersonic Σ-surface. One has been implemented at *NASA Langley Research Center*, based on the so-called *marching cubes algorithm* [44]. The other (named *K-Algorithm*) was developed by the first author. It evaluates the emission surface through the identification of patches of the supersonic regions and the use of a self-adaptive scheme which refines the numerical grid at each time step [45]; this algorithm has been recently improved in order to treat complex geometries and reduce the requested CPU time [46]. Figure 5 shows the agreement between the experimental data and the *HSI* (high speed impulsive) noise prediction achieved by K-Algorithm for a typical test-bed: the UH-1H hovering test case at a tip Mach number of 0.90; the numerical signature reproduces the asymmetrical shape of the measured waveform (due to the shock delocating off the blade tip) and provide an accurate evaluation of the peak acoustic pressure [43].

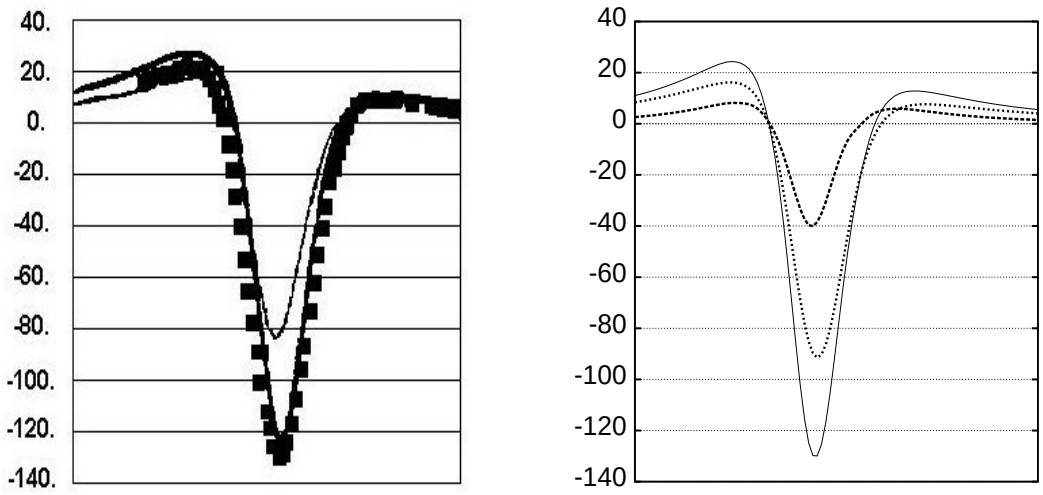

Figure 4: Comparison between the CAA (Euler) and the predictions based on the FWH equation for the UH-1H hovering rotor blade at M_{tip}=0.85 (non-delocating shock).

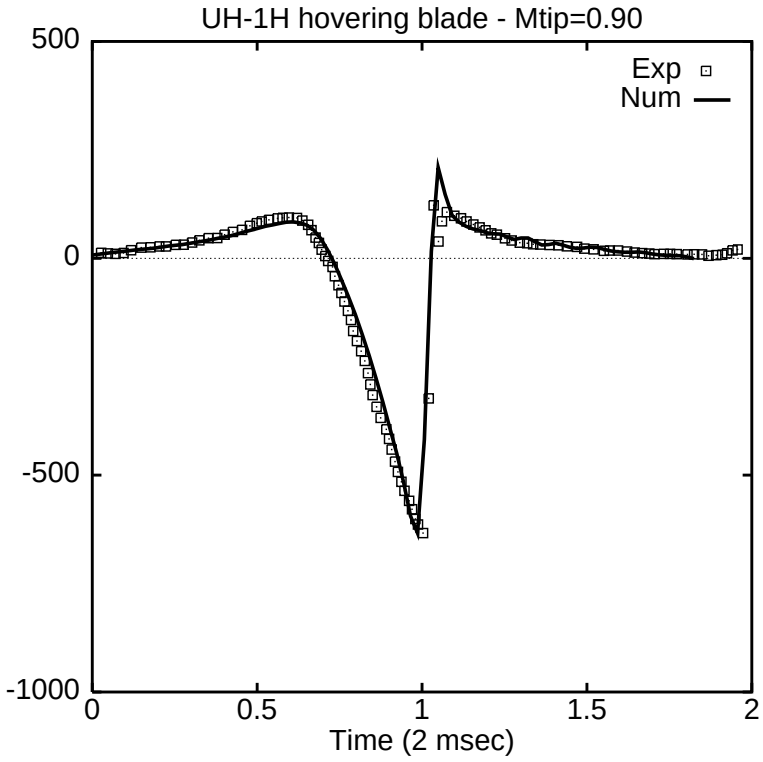

Figure 5: HSI noise prediction for the UH-1H hovering rotor blade at $M_{\text{tip}} = 0.90$ (delocating shock) using the K-Algorithm and the integration on a supersonic emission surface.

5 Hydroacoustics of marine propeller

The different density and the corresponding variation of the sound speed between air and water do not affect the main features of sound generation and propagation in the two fluids. Besides, the directivity pattern of the three sources is preserved, so they exhibit quadrupole, dipole and monopole behaviour, respectively. However, the usual operating conditions of a marine propeller — along with the very high speed of sound in water — prevent any possibility of shock wave to appear in the flow. Thus, significant effects of the non-linear (quadrupole) source term of the FWH equation may be related here to the turbulence and the mutual interactions between the propeller and the hull wake. Within this context, the most relevant difference between an aeronautical and a marine propeller is the possible occurrence of cavitation. This is a dynamic phenomena characterized by cavities filled with vapor, generated within the flow where the pressure falls to the vapor pressure of the fluid. Cavitation is responsible for a loss in the propeller thrust, erosion of the blade surface, vibration and noise.

In the case of marine propellers, cavitation-induced noise is mostly generated by attached cavitation on the blade surface (*sheet* cavitation) and by trailing vortex cavitation [47]. In particular, intermittent sheet cavitation in marine propellers operating in the wake of a ship hull is responsible for pressure pulses that may peak orders of magnitude larger than those generated in non-cavitating flow conditions. Current approach to the study of marine propeller sheet cavitation is mostly based on lifting-surface theory, while boundary-element methods are widely used in computation.

In the application presented here, a boundary element method for the velocity potential that is valid for inviscid incompressible flow is coupled with a non-linear sheet cavitation model. The cavity is determined as a region attached to the propeller blade surface where the pressure is constant and equals the vapor pressure (dynamic boundary condition). Using Bernoulli theorem, the constant pressure condition is recast in terms of velocity potential. Thus, a mixed Dirichlet/Neumann problem is solved for the velocity potential, where the potential is known on the cavity surface from the dynamic boundary condition, whereas the normal derivative of the potential is known on the wetted portion of the propeller surface from a non-penetration condition. Solving for the flow field requires the location of cavity to be known. This is achieved by an iterative process where an initial guess for the cavity is suitably prescribed. A numerical solution is obtained by a zero-th order boundary element approach.

From the sheet cavitation model, cavity extension and thickness are determined and used as the input for the hydroacoustic analysis. The present approach is capable to include either a trailing wake-alignment technique and a viscous-flow correction by means of a boundary-layer/potential-flow coupling technique. Details on the theoretical model addressed here may be found in [48], for non-cavitating flows, and in [49] for cavitating flows.

In order to test the capabilities of the formulations based on the FWH equation in computing the noise from a marine propeller, a new code (named MAPRA: MArine PRopeller Acoustics) has been developed. Unlike the usual solvers for aeronautical applications (where the geometry of the body does not change during the revolution period and the kinematics of the problem can be treated analitically), the blade-bubble configuration is required at several azimuthal positions (in the "water frame of reference"), in order to take into account the cavitation pattern. In fact, the occurrence of the cavity upon the blade surface corresponds, in practice, to a x-coordinate time variation at some nodes of the numerical grid; this means that an analytical description of the motion is not available and both the present and the retarded quantities must be determined through a suitable interpolation of the input data.

To check the reliability of the new procedure and to compare the predictions of noise at cavitating and non-cavitating conditions an isolated DTRC 4148 three-bladed propeller has been considered. The results shown here were presented in [50]. The hydrodynamic solution has been obtained on a numerical grid of 12 spanwise stations and a leading edge-stretched distribution of 72 nodes along chord; the diameter of the blade was set to 0.305 meters, with an advance ratio $J = 0.91$ (corresponding to an advance velocity for both the propeller and the observer of 4.775 m/s), a rotational speed of 1030.2 rpm and a cavitation number $\sigma_p = 2.757$.

An azimuthal step of 6° degrees was used for the evaluation of the blade airload and the time variable geometry of the sheet bubble, while the acoustic pressure time histories were determined by covering a complete revolution period with 2048 time steps. Note that, due to the periodicity of phenomena, the hydrodynamic solution was determined on the actual three-bladed model (thus accounting for the mutual interference between the blades), while the noise predictions always concern a single blade; this way it is possible to better appreciate the influence of sheet cavitation on the noise signature and to compare the numerical results at the different operating conditions.

Four microphones positions are selected, to test noise prediction capability. In fact, microphones 1 and 2 are located in the propeller plane where the thickness noise should be dominant, whereas microphones 3 and 4 are positioned downstream and upstream the propeller disk plane, respectively: at these locations a significant contribution from the loading term is expected. Figure 6 shows a 3D view of the DTRC 4148 propeller and highlights the microphone locations.

The hydrodynamic solution is determined on the actual three-bladed model (thus accounting for the mutual interference between the blades), whereas, by flow periodicity, noise predictions always concern a single blade. This allows to better appreciate the influence of sheet cavitation on the resulting noise waveform and to compare the numerical results at the different operating conditions.

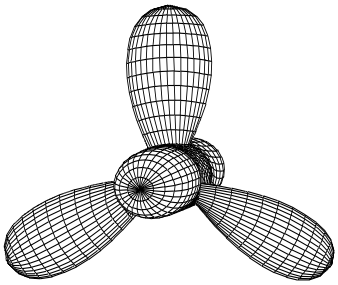

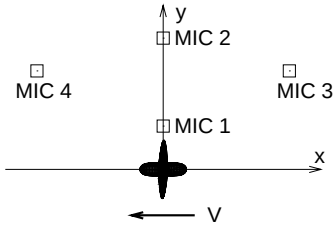

Mic.	x/D	y/D	z/D
1	0.00	0.66	0.00
2	0.00	2.00	0.00
3	2.00	1.50	0.00
4	-2.00	1.50	0.00

Figure 6: Three-dimensional view of the computational grid for the DTRC 4148 propeller and schematic of the microphone locations (with corresponding coordinates) for noise prediction tests.

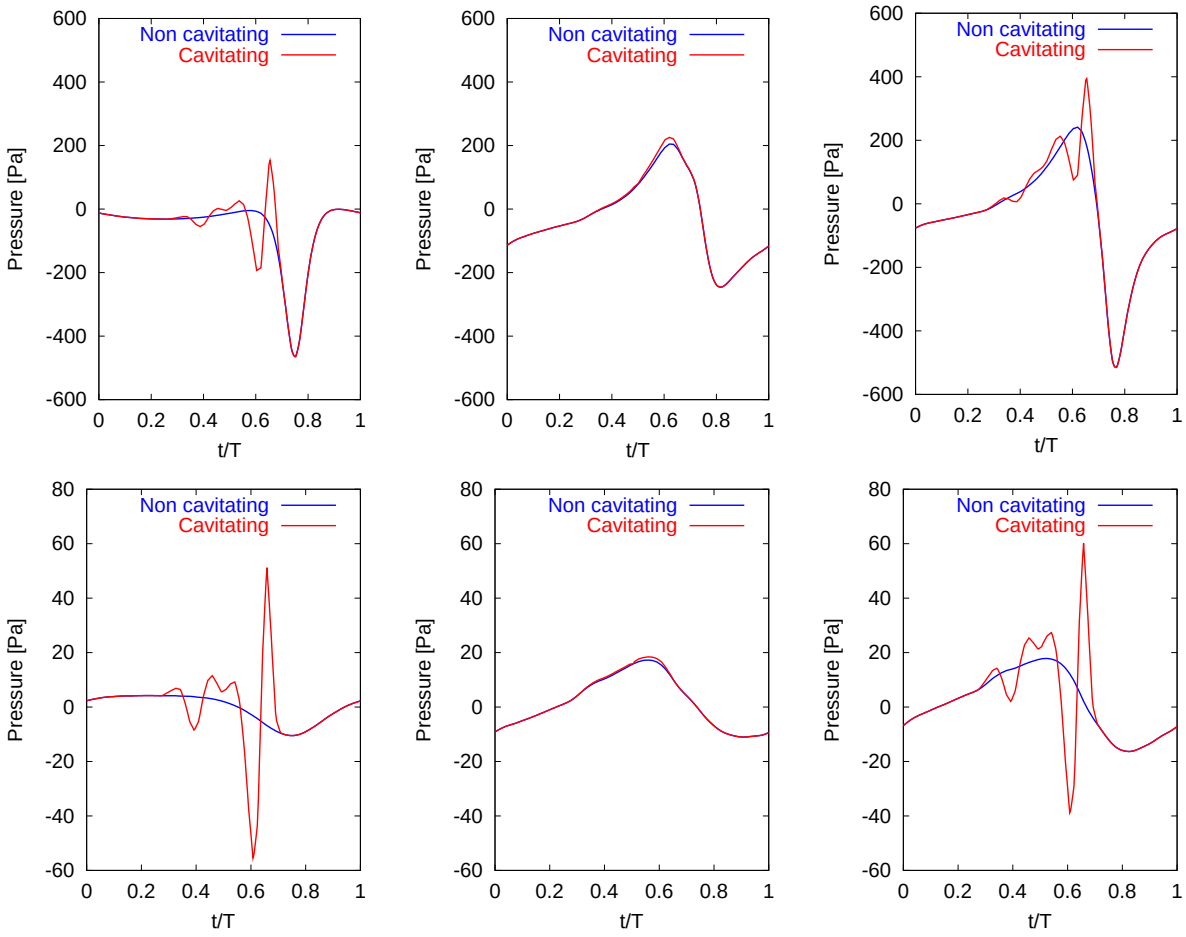

Figure 7: Comparison between noise predictions for cavitating and non-cavitating conditions: thickness (left), loading (center) and overall (right) signatures, at in-plane microphone locations 1 (top) and 2 (bottom).

Figure 7 shows noise predictions at the prescribed in plane locations (microphones 1 and 2). At each location the comparison between cavitating and non cavitating conditions is reported for the thickness and loading noise components, and for the overall noise signature. Looking at the non cavitating results of position 1 (very close to the blade tip) the noise signatures are as expected: at in plane locations the thickness noise exhibits a symmetrical shape and the high peak pressure, while the loading term has a typical waveform with smaller peak values. Relevant differences at cavitating conditions arise from the thickness noise: the occurrence of sheet cavitation gives the waveform an impulsive character. On the contrary, the loading noise does not seem to be influenced by vaporization, except for a little pressure increase at the angular positions affected by the cavity. Moving far from the blade tip (microphone 2) the thickness contribution is comparable with the loading noise and the relative difference between cavitating and non cavitating flow has a remarkable increase. The cavitation influence on the loading noise remains negligible, while the thickness noise is significantly affected, with consequences on the overall noise signature.

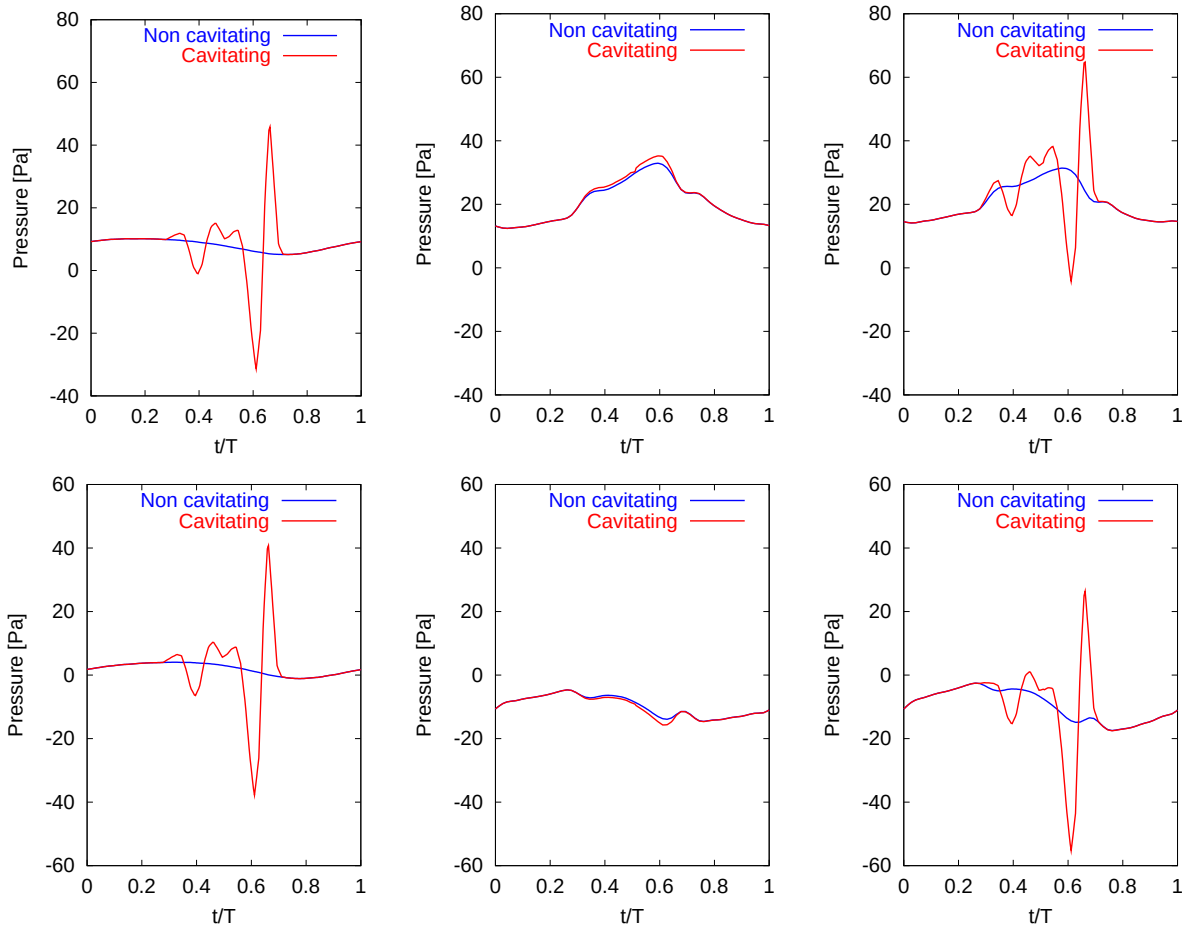

Figure 8: Comparison between noise predictions for cavitating and non-cavitating conditions: thickness (left), loading (center) and overall (right) signatures, at off-plane microphone locations 3 (top) and 4 (bottom).

These features become even more evident by moving far from the propeller disk plane, as shown in figure 8 where the results at microphones 3 and 4 are reported. Out of plane the loading term is predominant with respect to the thickness noise contribution generated by the (non cavitating) blade, but the occurrence of the sheet bubble deeply change the resulting noise waveform. Due to the symmetrical location of these microphones with respect to the propeller plane, the thickness component at non cavitating condition is practically the same, while the loading term rightly exhibits a sign inversion. Nonetheless, a very similar thickness noise waveform arises at the two different positions also at cavitating condition, even though the presence of the vapor sheet is limited to the upper surface of the blade; this result points out the actual monopole behaviour of the bubble, which acts as a pulsating sphere with a 3D homogeneous influence around the body. Noise predictions via the FWH equation confirm the monopole character of sheet cavity generated sound. The negligible influence on the loading noise component is reasonable, since the pressure time histories of each source point is not heavily affected by the occurrence of cavitation. On the contrary, source-body (blade plus vapor sheet) geometry and the corresponding normal velocity to the body surface rapidly change during the revolution period, thus explaining the higher frequency content and the impulsive character of the resulting noise signatures.

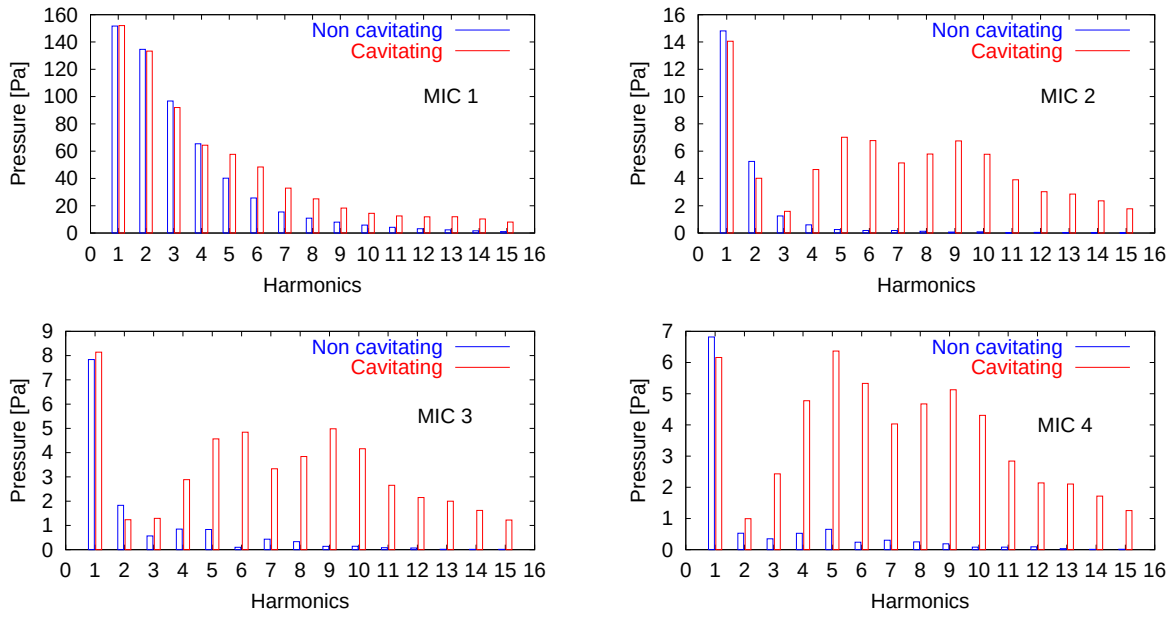

Figure 9: Comparison between predicted overall noise spectra for cavitating and non-cavitating conditions at the four microphone locations.

Finally, figure 9 focuses on the overall acoustic pressure spectra, showing the main difference between non cavitating and cavitating conditions: in the latter case, the impulsive character of the pressure waveform is reflected into significant spectrum components at higher harmonics of the blade passing frequency.

Part III

Conclusions

6 Concluding remarks on theoretical formulas

Advances in the application of the Kirchhoff method in discrete frequency noise prediction have been reviewed. Much progress has been made in the past thirty years. It can be said that for aeroacoustic applications one can depend exclusively on the FWH equation with a penetrable data surface enclosing the most significant part of the quadrupole sources.

The state of noise prediction for subsonic sources is highly satisfactory. When part or all of the data surface moves at supersonic speed, both the structure of the acoustic field and the mathematics become much more complicated. Part of the mathematical problem is due to the appearance of singularities in the analytic results which are not real. There is also cancellation of singularities among various integrals. Much progress has been made in the supersonic case, but a lot more is to be explored about this problem in the future.

7 Considerations on computational noise prediction

This paper deals with the capabilities and applications of the FWH equation in aeroacoustics and hydroacoustics. A limited overview of well-known results obtained in the past has shown why these methodologies are presently considered a standard resolution approach in the aeronautical context, especially for helicopter rotors and propellers. Due to the robustness of the FWH equation (derived from basic conservation laws) and the similarities of the problems, the same formulation has been applied to the hydroacoustic problem of noise prediction from a marine propeller, by taking into account for the possible occurrence of cavitation. Despite the absence of any comparison with experimental data, the noise predictions seem to exhibit reasonable features.

The presence of sheet cavitation deeply changes the acoustic pressure field: the air sheet behaves as a sort of monopole term, with an homogeneous, three dimensional radiation of sound around the propeller. Thus, the thickness noise contribution assumes an impulsive waveform with the introduction of high frequency components, while the loading term is just slightly affected by the phenomena and the overall noise signature exhibits a notable, increase especially in the far field.

Acknowledgements

This work has been supported by the Italian Ministry of Infrastructures and Transport, under the *INSEAN Research Programme 2000-2002*.

References

[1] F. Farassat, Acoustic radiation from rotating blades — The Kirchoff method in aeroacoustics. Journal of Sound Vibration, 239/4 (2001) 785-800 [obtainable from http://techreports.larc.nasa.gov/ltrs/PDF/2001/jp/NASA-2001-jsv-ff.pdf].

[2] L. Gutin, On The sound field of a rotating propeller. Original in Russian, in Zhurnal Tekhnicheskoi Fiziki, 12 (1936) 76-83, translated as NACA TM 1195 (1948).

[3] W. Ernsthausen, The source of propeller noise. Original in German, in Luftfahrtforschung 13(12) (1936), translated as NACA TM 825 (1937).

[4] A.F. Deming, Noise from propellers with symmetrical sections at zero blade angle, I. NACA TN 605 (1937).

[5] A.F. Deming, Noise from propellers with symmetrical sections at zero blade angle, II. NACA TN 679 (1938).

[6] M.V. Lowson, The sound field for singularities in motion. Proceedings of the Royal Society of London, A286 (1965) 559-572.

[7] M.J. Lighthill, On sound generated aerodynamically, I: general theory. Proceedings of the Royal Society, A211 (1952) 564-587.

[8] N. Curle, The influence of solid boundaries on aerodynamic sound. Proceedings of the Royal Society of London, A231 (1955) 505-514.

[9] J.E. Ffowcs Williams, D.L. Hawkings, Sound generation by turbulence and surfaces in arbitray motion. Philosophical Transactions of the Royal Society of London, A264 (1969) 321-342.

[10] I.M. Gelfand, G.E. Shilov, *Generalized Functions. 1: Properties and Operations*. Academic Press (1964).

[11] D.S. Jones, *The Theory of Generalized Functions. Second Edition*. Cambridge University Press (1982).

[12] R.P. Kanwal, *Generalized Functions — Theory and Technique*. Academic Press (1983).

[13] D.S. Jones, *The Theory of Electromagnetism*. Pergamon Press (1964).

[14] M.E. Goldstein, *Aeroacoustics*. McGraw-Hill (1976).

[15] F. Farassat, *Introduction to generalized functions with applications in aerodynamics and aeroacoustics*. NASA Technical Paper 3428 (1994) [corrected copy (April 1996) obtainable from http://techreports.larc.nasa.gov/ltrs/PDF/tp3428.pdf].

[16] F. Farassat, *The Kirchhoff formulas for moving surfaces in aeroacoustics — The subsonic and supersonic cases*. NASA Technical Memorandum 110285 (1996) [obtainable from http://techreports.larc.nasa.gov/ltrs/PDF/NASA-96-tm110285.pdf].

[17] F. Farassat, M.K. Myers, Extension of Kirchhoff's formula to radiation from moving surfaces. Journal of Sound and Vibration, 123 (1988) 451-560.

[18] P. di Francescantonio, A new boundary integral formulation for the prediction of sound radiation. Journal of Sound and Vibration, 202/4 (1997) 491-509.

[19] K.S. Brentner, F. Farassat, An analytical comparison of the acoustic analogy and Kirchhoff formulation for moving surfaces. AIAA Journal 36/8 (1998) 1379-1386 [obtainable from http://techreports.larc.nasa.gov/ltrs/PDF/1998/jp/NASA-98-aj-ksb.pdf].

[20] D.G. Crighton, A.P. Dowling, J.E. Ffowcs Williams, M. Heckl, F.G. Leppington, *Modern Methods in Analytical Acoustics*. Lecture Notes, Springer-Verlag (1992).

[21] A.D. Pierce, *Acoustics: an Introduction to its Phisical Principles and Applications*. McGraw-Hill (1981).

[22] P.M. Morse, H. Feshbach, *Methods of Theoretical Physics*. McGraw-Hill (1953).

[23] N. Bleistein, *Mathematical Methods for Wave Phenomena*. Academic Press (1984).

[24] F. Farassat, K.S. Brentner, The uses and abuses of the acoustic analogy in helicopter rotor noise prediction. Journal of the American Helicopter Society, 33/1 (1988) 29-36.

[25] F. Farassat, *Theory of noise generation from moving bodies with an application to helicopter rotors*. NASA Technical Report R-451 [obtainable from http://techreports.larc.nasa.gov/ltrs/PDF/NASA-75-trr451.pdf].

[26] F. Farassat, Linear acoustic formulas for calculation of rotating blade noise. AIAA Journal, 19/9 (1981) 1122-1130.

[27] F. Farassat, G.P. Succi, The prediction of helicopter rotor discrete frequency noise. Vertica, 7 (1983) 309-320.

[28] K.S. Brentner, *Prediction of Helicopter rotor discrete frequency noise — A computer program incorporating realistic blade motions and advanced acoustic formulation*. NASA Technical Memorandum 87721 (1986).

[29] F. Farassat, Theoretical analysis of linearized acoustics and aerodynamics of advanced supersonic propellers. AGARD Conference Proceedings 366 (1985).

[30] F. Farassat, S.L. Padula, M.H. Dunn, Advanced turboprop noise prediction based on recent theoretical results. Journal of Sound and Vibration, 119/1 (1987) 53-79.

[31] F. Farassat, M. Farris, The mean curvature of the influence surface of wave equation with sources on a moving surface. Mathematical Methods in Applied Sciences, 22/17 (1999) 1485-1503.

[32] E. De Bernardis, F. Farassat, On the possibility of singularities in the acoustic field of supersonic sources when BEM is applied to a wave equation. In: B.S. Annigeri and K. Tseng (Eds.), *Boundary Element Methods in Engineering*. Springer-Verlag (1990) 522-528.

[33] F. Farassat, M.K. Myers, Line source singularity in the wave equation and its removal by quadrupole source — a supersonic propeller noise problem. In: J.E. Ffowcs Williams, D. Lee and A.D. Pierce (Eds.), *Structural Acoustics, Scattering and Propagation*. International Conference on Theoretical and Computational Acoustics, Volume 1, World Scientific (1994) 29-43.

[34] F. Farassat, K.S. Brentner, M.H. Dunn, A study of supersonic surface sources — The Ffowcs Williams-Hawkings equation and the Kirchhoff formula. AIAA Paper 98-2375 (1998) [corrected copy obtainable from http://techreports.larc.nasa.gov/ltrs/PDF/1998/aiaa/NASA-aiaa-98-2375.pdf]

[35] J.W. Bruce, P.J. Giblin, *Curves and Singularities — Second Edition*. Cambridge University Press (1992).

[36] H. Ardavan, The breakdown of the linearized theory and the role of quadrupole sources in transonic rotor acoustics. Journal of Fluid Mechanics, 226 (1991) 591-624.

[37] A.S. Lyrintzis, Review, the use of Kirchhoff's method in computational aeroacoustics. ASME Journal of Fluids Engineering, 116 (1994) 665-676.

[38] S. Ianniello, Loading noise prediction using experimental data from HELINOISE test campaign at DNW. 20th European Rotorcraft and Powered Lift Aircraft Forum, Amsterdam, The Netherlands (1994) No. 112.

[39] S. Ianniello, *CIRA aeroacoustics effort within the IMT Project HELISHAPE*. CIRA TR-96-162, 1996.

[40] S. Ianniello, *Linear aeroacoustic analysis of the HELIFLOW helicopter configuration*. CIRA CR-01-090 (2001).

[41] J.D. Baeder, The role and status of Euler solvers in impulsive rotor noise computations. AGARD Symposium on Aerodynamics and Aeroacoustics of Rotorcraft, Berlin, Germany (1994) No. 33.

[42] S. Ianniello, E. De Bernardis, Calculation of high speed noise from helicopter rotor using different descriptions of quadrupole source. AGARD Symposium on Aerodynamics and Aeroacoustics of Rotorcraft, Berlin, Germany (1994) No. 27.

[43] S. Ianniello, Quadrupole noise predictions through the Ffowcs Williams-Hawkings equation. AIAA Journal, 37/9 (1999) 1048-1054.

[44] F. Farassat, K.S. Brentner, Supersonic quadrupole noise theory for high-speed helicopter rotors. Journal of Sound and Vibration, 218/3 (1998) 481-500.

[45] S. Ianniello, Algorithm to integrate the Ffowcs Williams-Hawkings equation on supersonic rotating domain. AIAA Journal, 37/9 (1999) 1040-1047.

[46] S. Ianniello, Aeroacoustic analysis of high tip-speed rotating blades. Aerospace Science and Technology, 5/3 (2001) 179-192.

[47] W.K. Blake, *Mechanics of Flow-Induced Sound and Vibration*. Academic Press (1986).

[48] P.G. Esposito, F. Salvatore, F. Di Felice, G. Ingenito, Experimental and numerical investigation of the unsteady flow around a propeller. Proceedings of the 23rd Symposium on Naval Hydrodynamics, Val de Reuil, France (2000).

[49] F. Salvatore, P.G. Esposito, An improved boundary element analysis of cavitating three-dimensional hydrofoils. Proceedings of CAV 2001, Fourth International Symposium on Cavitation, Newcastle upon Tyne, United Kingdom (2001) B1.006.

[50] F. Salvatore, S. Ianniello, Preliminary results on acoustic modelling of cavitating propellers. Proceedings of IABEM 2002, Symposium of the International Association for Boundary Element Methods, Austin, TX, USA (2002) 4.3.